

Relationship of concretions and chlorite–muscovite porphyroblasts to the development of domainal cleavage in low-grade metamorphic deformed rocks from north-central Wales, Great Britain

BERTRAM G. WOODLAND

Department of Geology, Field Museum of Natural History, Roosevelt Road at Lake Shore Drive,
Chicago, IL 60605, U.S.A.

(Received 23 January 1984; accepted in revised form 13 August 1984)

Abstract—Spaced or domainal cleavage is widespread in deformed rocks of low metamorphic grade. This study presents evidence on the origin of spaced cleavage in deformed pelites from Silurian turbidite sequences in north-central Wales. The variable development of cleavage folia is related to the presence of concretions, which served to concentrate strain effects of well-developed cleavage folia in the matrix in some zones and to produce 'strain shadows' (few or no cleavage folia) in others. Compositional differences between matrix, narrow transition zones, and concretions also influenced the development of cleavage folia. Chlorite–muscovite porphyroblast growth was initiated before cleavage formation, but its further growth and development took place during cleavage formation. The relationship of cleavage to the concretions and to the chlorite–muscovite porphyroblasts indicates that cleavage developed in a matrix that must have been in an advanced state of lithification (anchimetamorphic to lowermost greenschist facies of metamorphism) and not during soft-sediment deformation.

INTRODUCTION

Pelitic and semi-pelitic domainal cleavage development

WIDESPREAD development of spaced or domainal cleavage as a secondary structure in deformed pelitic rocks of low metamorphic grade is now amply documented (e.g. Williams 1972, Gray 1978, White & Knipe 1978, Woodland 1982). Spaced cleavage is characterized by parallel folia of phyllosilicates separated by microlithons of contrasting mineralogy, usually quartz, feldspar and calcite, with sparse phyllosilicates commonly oriented at a high angle to the cleavage folia. The degree of cleavage development in lithologically similar rocks may vary on a scale of a few centimeters (Talbot 1965, Knipe & White 1977, Woodland 1982) to kilometers (Piqué 1982, Reks & Gray 1983). Evolution of a penetrative slaty cleavage or a closely spaced cleavage from crenulation cleavage and from crenulations of a precursor preferred orientation of phyllosilicates is also well established (Williams 1972, Knipe & White 1977, Gray 1978). The precursor preferred orientation may have been a depositional or compactional structure parallel to bedding, or it may have been a cleavage formed during a preceding deformation.

Cleavage in pelitic or semi-pelitic rock with no preferred orientation of phyllosilicates cannot develop in such a manner. Instead, short zones of pressure solution are probably initiated at heterogeneities under the influence of stress gradients (Cobbold 1977). The mass transfer results in permanent deformation by the removal of some constituents, perhaps more in certain microdomains than in others (Plessman 1964, Groshong 1975, Beach 1979), and in crystallization of new grains, particularly phyllosilicates (Stephens *et al.* 1979, Knipe 1981, White & Johnson 1981). Grain-boundary sliding and minor grain rotation accompany mass removal and

result in passive accumulation of insoluble material along developing phyllosilicate-rich folia (Woodland 1982). End propagation of these folia leads to longer folia and coalescence into more continuous cleavage domains. Continuation of the process, possibly catalyzed by enhanced grain-boundary fluid movements along the folia, produce thicker cleavage folia and reduction in width of the microlithons. The latter may also be the site of crystallization of some constituents; for example, 'strain-shadow' grains in extension sites (parallel to the extension direction) and characteristic lozenge- and barrel-shaped chlorite–muscovite porphyroblasts (Woodland 1982).

Porphyroblasts in pelites and semi-pelites

Chlorite porphyroblasts, generally intergrown with white mica, are characteristic of low-grade pelitic rocks. A common feature, particularly in rocks with a well-developed domainal cleavage, is the orientation of the porphyroblasts' {001} basal planes at a high angle to the cleavage folia and the confining of these porphyroblasts between two folia. Such porphyroblasts have a barrel or lozenge shape; their dimension normal to {001} may equal or exceed the dimension parallel to {001}.

Purpose of this paper and methods of work

I have examined weakly cleaved siltstone and argillaceous rock as well as slate containing calcareous or siliceous concretions from Silurian turbidite sequences of north-central Wales in order to (1) ascertain the time of their cleavage development relative to development of the concretions, (2) evaluate the influence of concretion lithology on the distribution and nature of the cleavage folia and (3) determine whether the chlorite–muscovite porphyroblasts exhibit any relation-

ship to the development of cleavage folia in both matrix and concretions.

This paper is not intended to describe in detail north-central Wales cleavage nor its origin, but, rather, to compare the relationship of porphyroblast shape to the relative strength of cleavage development and to examine the development of spaced cleavage in relation to early diagenetic concretions (for a discussion of cleavage development *per se*, see Woodland 1982).

Porphyroblast geometry has been recorded from data drawn from thin sections cut perpendicular to both cleavage and bedding. Only in such sections can the orientations of the same grains relative to both bedding and cleavage be measured, a general requirement of the study. Sections cut normal to this plane in analogous specimens confirmed my geometrical observations. Sections cut normal to cleavage and normal to the section plane used tend to show relatively few porphyroblasts because the {001} cleavages lie nearly parallel with the section and the 'cut-effect' reduces the intercepts. Few useful orientations relative to cleavage or thickness of the porphyroblasts could be measured. Sections parallel to cleavage show chlorite stacks similar to the first orientations. However, no measurement could be made relative to cleavage, and bedding was not normal to these slices.

Because of the small grain size, I used a scanning electron microscope to examine several of the concretions as well as the rock matrix, and found the S.E.M. helpful in identifying framboidal pyrite. In the future it is planned to examine the porphyroblasts with an S.E.M. energy dispersive analyzer and electron microprobe analyzer.

RELATIONSHIP OF CONCRETIONS TO CLEAVAGE DEVELOPMENT

The Nantglyn Flags are composed of a sequence of banded siltstone and mudstone, sometimes with carbonate or siliceous ovoid concretions (Boswell 1949, Cummins 1959). The concretions have their longest

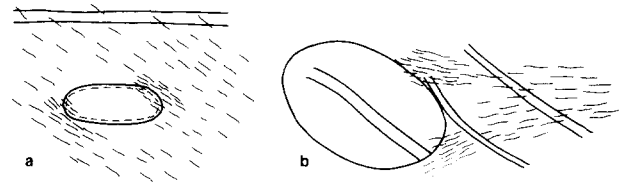


Fig. 1. Diagrammatic representation of bedding and cleavage folia relationships to ovoid concretions in the Nantglyn Flags. The short lines represent folia: the continuous lines represent bedding. Note increase of folia in matrix adjacent to concretion, few or no folia within concretion, and absence of folia in 'shadow zones' in matrix near concretion. (a) Specimen Li 9591; 1832. Length of calcareous concretion parallel to bedding = 30 mm. (b) Specimen Li 9596; 1838. Length of siliceous concretion parallel to bedding = 50 mm.

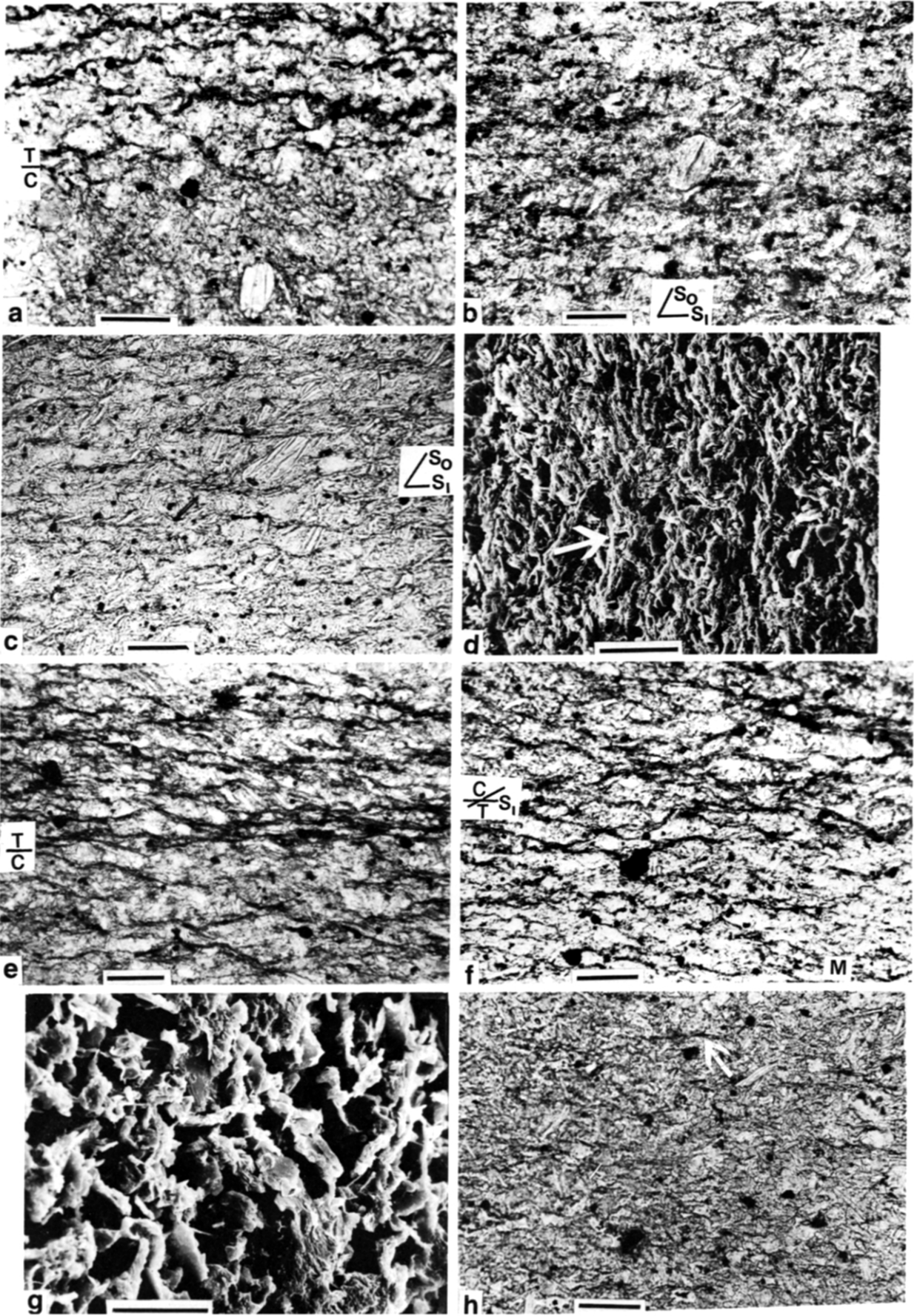
dimension parallel to bedding; lengths range from 27 to 100 mm, thicknesses from 13 to 60 mm. The bedding traces above and below them curve around so that the distance between the traces decreases laterally from the concretions. Within the concretions the silty layers are thicker and have more irregular boundaries than outside the concretions. These bedding relationships are shown diagrammatically in Fig. 1. The concretions contain undeformed molds of a cephalopod and a possible brachiopod; no shell remains, but the molds are partially or completely filled with coarse calcite.

These aspects indicate a pre-compactional early diagenetic origin for the concretions. If concretions form early in diagenesis, their fabric and bulk composition will contrast with those of the surrounding matrix. The matrix will experience compaction as well as diagenetic changes during and following formation of the concretions.

Nantglyn Flags with carbonate concretions

A suite of Denbigh grit specimens was collected from a disused quarry in Lower Ludlow (Upper Silurian) Nantglyn Flags on the Denbigh Moors, some 10–15 km southwest of Denbigh (Nat. Grid SH 966604). The bedding here has a dip of 11° to the southeast. No minor folds are present in the outcrop.

Fig. 2. Photomicrographs of Nantglyn Flags with carbonate concretions; sections cut normal to cleavage and bedding. (a) Specimen Li 9588; 1827. Transition zone (top: T) with prominent undulatory cleavage folia at boundary between matrix and concretion (bottom: C). Folia are parallel (or nearly parallel) to the concretion margin; the concretion has no folia. The matrix (not shown) has only widely spaced, short, thin folia at a high angle to bedding. Note chlorite–muscovite porphyroblast in concretion. Scale bar = 0.05 mm. (b) Specimen Li 9590; 1830. Fine-grained matrix; cleavage (S_1) is marked by short, parallel, spaced, thin folia, composed of phyllosilicates and fine opaque material, at an angle of 63° to bedding (S_0). Trace of {001} in chlorite porphyroblast is nearly parallel to bedding. Scale bar = 0.05 mm. (c) Specimen Li 9593; 1834. Fine-grained matrix with relatively well-developed cleavage folia (S_1) composed of phyllosilicates and opaque material; round, opaque pyrite framboids common. Long dimension of largest chlorite–muscovite porphyroblast is only 7° from bedding (S_0); cleavage folia are 57° from bedding. Scale bar = 0.05 mm. (d) Scanning electron micrograph (etched thin section): specimen Li 9591; stub 2(D6). Matrix shows phyllosilicates forming sinuous cleavage folia (arrow). Scale bar = 20 μ m. (e) Specimen Li 9590; 1830. Concretion (C) is at the bottom and matrix at the top; prominent cleavage folia are developed in transition zone (T) parallel to boundary of concretion and normal to bedding [compare with (b), where folia in matrix are at an angle of 63° to bedding.] Scale bar = 0.05 mm. (f) Specimen Li 9591; 1832. Well-developed cleavage folia (S_1) in transition zone (T) between concretion (C) and matrix (M); concretion in top left corner. Cleavage lies at 28° to concretion boundary and 38° to bedding in matrix. Note reduction in number of folia in concretion and in matrix away from boundary. Scale bar = 0.05 mm. (g) Scanning electron micrograph (etched thin section); specimen Li 9591; stub 2(D6). Concretion showing phyllosilicates with no development of cleavage folia. Scale bar = 20 μ m. (h) Specimen Li 9593; 1834. Concretion area showing weak development of cleavage (horizontal: arrow) as short, widely spaced folia of phyllosilicates and opaque material. Folia are at an angle of 71° to bedding in matrices, which is not shown in the figure. Scale bar = 0.05 mm.



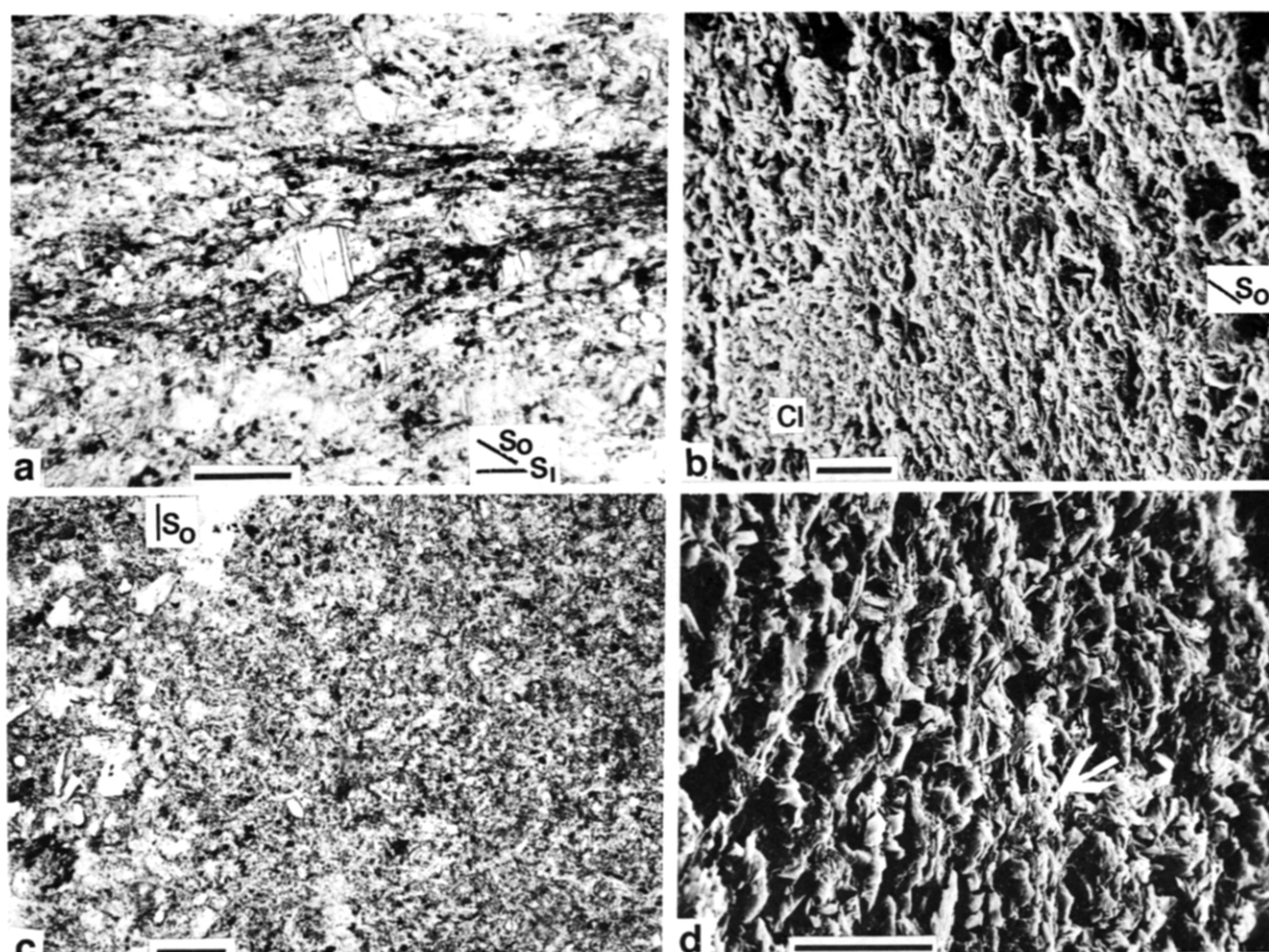


Fig. 3. Photomicrographs of specimen Li 9596, Nantglyn Flags with siliceous concretion; sections cut normal to cleavage and bedding. (a) Thin section 1838. Bedding (S_0) trace runs diagonally from top left to bottom right. Cleavage folia (S_1) composed of phyllosilicates and opaque material, including aligned pyrite framboids developed in silty shale of the matrix at an angle of 29° to the bedding. Trace of {001} of the chlorite–muscovite porphyroblast is nearly normal to cleavage and 54° to bedding. Scale bar = 0.1 mm. (b) Scanning electron micrograph; stub 2(D10). Silty shale matrix showing phyllosilicates in well-developed cleavage, approximately N–S. Bedding (S_0) trace runs from top left to middle right. Note chlorite porphyroblast (Cl) in lower left corner. Scale bar = $30\ \mu\text{m}$. (c) Thin section 1838. Concretion composed essentially of very fine-grained quartz, randomly oriented phyllosilicate grains, and opaque grains, including pyrite framboids. Bedding (S_0) indicated by coarser-grained quartz on left. Scale bar = 0.1 mm. (d) Scanning electron micrograph; stub 2(E1). Transition zone between siliceous concretion and matrix, with phyllosilicates forming cleavage folia (arrow). Scale bar = $20\ \mu\text{m}$.

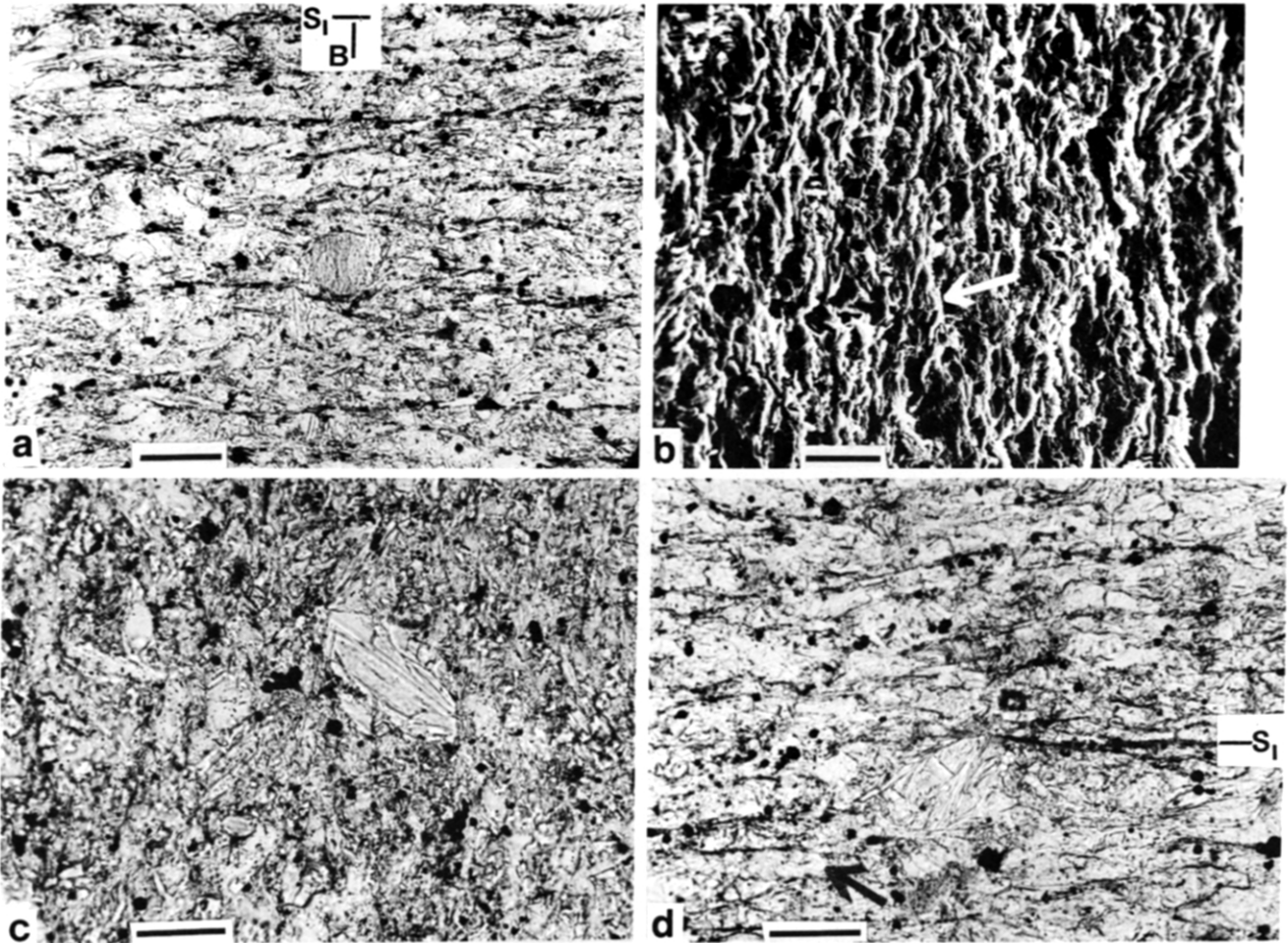


Fig. 4. Photomicrographs of Specimen Li 9604, Lower Ludlow Slate with carbonate concretion; sections cut normal to cleavage and bedding. (a) Thin section 1853. Spaced cleavage folia (S_1) in fine-grained, quartz-rich matrix lateral to concretion. Carbonate grains are common in the microlithons; opaque grains include pyrite framboids. Note traces of $\{001\}$ (B) of chlorite porphyroblast at a high angle to folia. Scale bar = 0.05 mm. (b) Scanning electron micrograph; stub 2(E2). Etched thin section of matrix showing prominent orientation of phyllosilicates in cleavage folia (arrow). Scale bar = 20 μm . (c) Thin section 1853. From region vertically above (or below) the middle of the concretion ('shadow zone'). Matrix of quartz, carbonate, phyllosilicates, and opaque grains, with no development of cleavage folia. Note elongate chlorite–muscovite porphyroblast. Scale bar = 0.05 mm. (d) Thin section 1853. Cleavage folia (S_1) within lateral boundary of concretion and near transition zone. Some calcite grains (arrow) are elongate parallel to the cleavage. Scale bar = 0.05 mm.

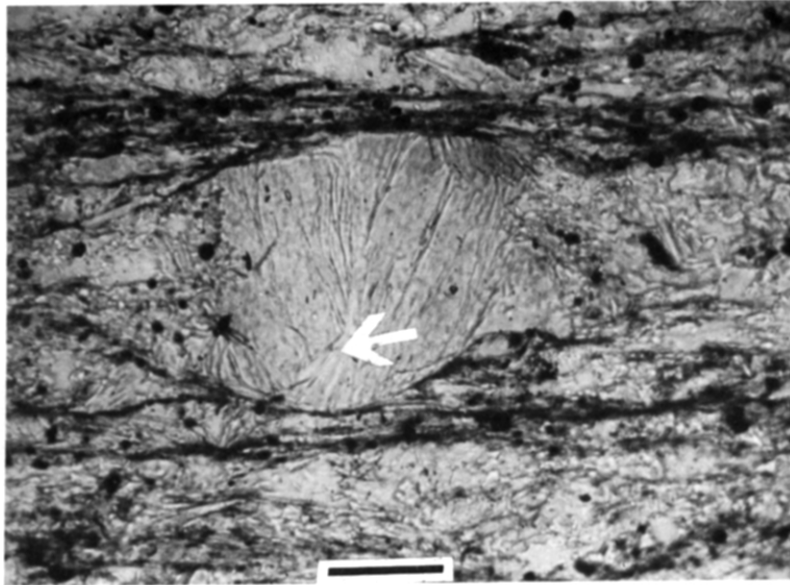


Fig. 5. Photomicrograph of chlorite-muscovite porphyroblast in matrix near the transition zone, Lower Ludlow Slate, Specimen Li 9604; 1853. Arrow indicates white mica laminae. Note cleavage folia at a high angle to {001} and tightly against the porphyroblast; pyrite framboids aligned, in part in folia. Scale bar = 0.05 mm.

The siltstone layers are quartz-rich, with quartz grains 0.02–0.05 mm (rarely to 0.1 mm) in diameter. Fine-grained interstitial phyllosilicates make up folia 4 μm thick and spaced 0.04–0.09 mm apart. They occur with much opaque material (0.015–0.03 mm), including aggregates of framboidal pyrite. Some larger muscovites have their {001} cleavage generally oriented approximately parallel to bedding (S_0). Minor calcite (0.04 mm across) is present in some specimens. Plagioclase is rare.

The finer-grained mudstones contain abundant tiny phyllosilicates (1–6 μm wide, 19–25 μm long) which have a preferred orientation approximately parallel to bedding; quartz (generally 0.02 mm in diameter) is common. Opaque materials occur as small grains, very fine particles, and framboids (up to 4 μm). Chlorite–muscovite composite porphyroblasts (20–40 μm long) are sparse in some specimens and common in others; their {001} cleavage tends to be oriented parallel to bedding.

The seven carbonate concretions studied are composed of abundant, very fine grained calcite (mostly 2–5 μm in diameter), with sparse quartz, sparse phyllosilicates, and opaque material, including framboids. Chlorite–muscovite grains (20–40 μm long) are sparse to rare.

Cleavage folia are variably developed in the siltstones and mudstones. Generally the rocks exhibit no macroscopic cleavage, but only a very weak spaced cleavage. In thin section, however, folia are evident in most specimens. All of the cleavage folia are composed of opaque material (mainly fine dust-like material, but including larger grains and framboids) and of phyllosilicates oriented with their {001} planes approximately parallel with the folia. In all of the specimens cleavage folia are found near the boundary of concretions (e.g. Figs. 1a and 2a). In some samples these folia are all that are present. In others there is a weak development of folia in the matrix (Fig. 2b); these folia are so very short, thin (1–4 μm), and widely scattered (up to 40 μm apart) that there is no continuous cleavage whatsoever. Some folia may be longer, thicker (up to 5 μm), and closer-spaced (15 μm), (Figs. 2c and d). In the coarser quartz-rich siltstone layers the folia are short, wavy, and with a crude cleavage similar to Gray's (1978) 'rough cleavage'.

Cleavage folia are prominently developed (Figs. 1a and 2e) in the zone adjacent to a concretion where the concretion boundary is nearly parallel with, or at a relatively low angle to, the folia in the matrix (but away from the influence of the concretion). The folia curve to conform partially to the boundary of the concretion. The zone is narrow, usually less than 0.4 mm wide and rarely as much as 1.0 mm. The cleavage folia are commonly well-developed in this zone, but diminish in thickness, while their spacing increases both into the concretion and into the matrix.

The interiors of the concretions generally lack folia (Fig. 2g), but in some cases they may contain some folia for a short distance (about 1.15 mm) adjacent to the margin section where the folia are more strongly developed in the transition zone or matrix (Fig. 2f). In

two samples (Li 9593, Li 9594) very weak folia, short, less than 2 μm thick, and widely spaced, occur within the concretion (Fig. 2h).

Nantglyn Flags with siliceous concretions

Several somewhat weathered siliceous concretions with matrix were collected from a low, very weathered outcrop (Nat. Grid. SH 925570) some 5 km southwest of the old quarry where the Nantglyn Flag specimens with carbonate concretions were collected. Macroscopically the rocks are quite similar to the first suite.

The silty shale of the matrix is composed of thin layers with coarse grains of quartz (up to 0.05 mm) alternating with fine-grained layers of abundant small phyllosilicates, common quartz (up to 0.02 mm), and framboids. Chlorite–muscovite composite porphyroblasts (34–42 μm long) are prominent in both types of layers. Cleavage folia are well-developed in the fine-grained layers (Figs. 3a and b); they are short, 1–2 μm thick, and spaced from 0.012 to 0.03 mm apart. Composed of phyllosilicates and heavily stained with opaque weathering products, these folia are prevalent enough to form a penetrative structure. In the coarser-grained layers cleavage folia are crude, heavily stained, up to 8 μm thick, and somewhat more widely spaced.

The concretions are essentially composed of a mosaic of quartz grains, most in the range of 4–8 μm in diameter with some up to 0.05 mm. Disseminated phyllosilicates have no apparent preferred orientation. Chlorite–muscovite grains (0.036 mm long) are sparse; there are some larger muscovite grains up to 0.045 mm long. Very tiny grains (2 μm and less) of carbonate are scattered throughout. Rhombs of iron oxide, after ankerite or siderite, occur in one specimen.

The concretion boundaries are difficult to discern in detail. There are no cleavage folia in the concretions (Fig. 3c), but in the boundary zone some folia are present (Fig. 3d) and increase in prominence into the matrix away from the concretions (Fig. 1b). The bedding shows an inflexion in the zone where cleavage folia are sparse; this marks a probable transition zone from the matrix to the concretion. Whether the silica of the concretions is original or replaces carbonate is not evident. The minute carbonate grains sprinkled within the concretions may be relict, suggesting a replacement origin for the silica.

Lower Ludlow Slate with carbonate concretions

A third set of specimens was collected from the strongly folded northern limb of the Llangollen syncline, as exposed in a slate quarry overlooking Horseshoe Pass, 7 km northwest of Llangollen (Nat. Grid SJ 183470).

The matrix of this Lower Ludlow Slate has well-developed cleavage folia, up to 4 μm thick and spaced some 16–35 μm apart, in some cases up to 50–60 μm apart (Figs. 4a & b). The microlithons are composed of abundant quartz (c. 0.02–0.06 mm in diameter), much

carbonate generally larger in grain size (up to 0.2 mm) than the quartz, and phyllosilicates with their {001} cleavages frequently at a high angle to the folia. Pyrite framboids are common, and chlorite–muscovite porphyroblasts (32 μm long) sparse to common (Fig. 5).

The carbonate content may increase abruptly into a well-defined concretion or increase gradually into a narrow (2–3 mm wide) transition zone. Such a transition zone has prominent folia, rarely as much as 8 μm thick and spaced c. 0.016–0.06 mm apart; the calcite grains are distinctly elongate parallel to the folia. The cleavage folia in the transition zone and adjacent matrix are poorly developed away from the lateral margins of the concretions and towards the middle in the upper and lower surfaces (Fig. 4c), that is, in the 'shadow zone' of the concretion.

Within the concretions, folia are either absent or very weakly developed as short (about 0.1 mm), thin (1–2 μm) lamellae, spaced some 0.028–0.08 mm apart (Fig. 4d). Some of the folia are more prominent (about 0.6 mm longer and up to 8 μm thick) but more widely spaced (0.15–0.45 mm apart). Carbonate is very abundant and fine-grained (c. 0.008–0.06 mm). Quartz is common. Muscovite is sparse, some oriented with {001} approximately parallel to bedding, and chlorite–muscovite porphyroblasts (31 μm long) are rare. Opaque grains and clots are common, many occurring as pyrite framboids. Coarse carbonate grains have nucleated and grown on the upper and lower surface of the opaque clots; in some

cases curved quartz fibers have grown in similar positions. Generally the direction of growth is approximately parallel to the cleavage folia.

RELATIONSHIP OF PORPHYROBLASTS TO CLEAVAGE DEVELOPMENT

Statistical studies of the shape and orientation of chlorites have shown that the orientation of {001} is not related to cleavage folia, but is generally near to bedding (Beutner 1978, Weber 1981, Craig *et al.* 1982, Woodland 1982).

The origin of porphyroblasts has been described as detrital (Beutner 1978), diagenetic (Craig *et al.* 1982, Woodland 1982), or syntectonic with cleavage formation (Talbot 1965, Roy 1978, Weber 1981). Beutner (1978) considered his detrital grains to have been modified in shape by syntectonic pressure solution perpendicular to the cleavage. Craig *et al.* (1982) referred to modification of shape of the diagenetic chlorite by syntectonic pressure solution as 'corrosion'.

Variation in shape and orientation of the porphyroblasts may reflect varying conditions of growth or dissolution and crystallization dependent upon location within a deforming rock mass, for example, on the limb or hinge of a developing fold or in layers of contrasting grain size, composition and rheological properties (Woodland 1982).

Table 1. Statistical data on chlorite–muscovite porphyroblasts

1	2	3	4	5		7	8		9		10			11			12			13			14			15			16			17			18			19		
				S ₁ ∠ to bed- ding	Number of grains		{001}L μm	{001}L/W ₁		L.D./W ₁	{001} ∠ bedding		{001} ∠ S ₁		{001} ∠ S ₁			L.D. ∠ S ₁			L.D. ∠ S ₁			L.D. ∠ S ₁			L.D. ∠ S ₁			L.D. ∠ S ₁			L.D. ∠ S ₁							
								All grains	Grains with L.D. not ∥ to {001}		+ or - angle	Simple angle	Simple angle	Minus angle	Simple Angle			L.D. ∠ {001}	L.D. ∠ {001}	Total L.D. not ∥ to {001}	Simple angle			L.D. ∠ {001}	L.D. ∠ {001}	Total L.D. not ∥ to {001}	L.D. ∠ S ₁													
															L.D. ∠ to {001}	L.D. at ∠ to {001}	L.D. not ∥ to {001}				L.D. ∠ to {001}	L.D. ∠ to {001}	Total L.D. not ∥ to {001}																	
Li 9591 Matrix	+42	171	30(12)	2.8(1.1)	1.97 (0.78) [10]	1.67(0.24) [10]	-15(23)	21(17)	54(19)	-56(23)	-	-	47(13) [10]	23 (7) [10]	-	-	24(14) [10]	26(23) [10]																						
	Matrix transition	+42	28	34(13)	3.2(1.8)	-	-	-9(15)	13(12)	50(15)	-50(15)	-	-	-	-	-	-	-																						
	Concretion	+56	81	30(13)	3.1(1.2)	-	-	-15(24)	21(18)	64(15)	-72(24)	-	-	-	-	-	-	-																						
Li 9593 Matrix	+70	146	31(12)	3.1(1.4)	2.13(0.73) [13]	1.82(0.27) [9]	-10(26)	22(17)	65(15)	-80(25)	-	-	60(19) [13]	21(20) [13]	-	-	52(15) [13]	33(18) [13]																						
	Matrix transition	+60	100	28(13)	2.8(1.3)	1.9 (0.75) [8]	2.0 (0.55) [8]	0(27)	21(16)	55(20)	-61(28)	-	-	57(11) [8]	23 (8) [8]	-	-	34(10) [8]	35(23) [8]																					
	Concretion	+70	62	31(12)	3.5(1.6)	-	-	-6(23)	20(14)	69(16)	-76(23)	-	-	-	-	-	-	-																						
Li 9596 Matrix	-53	195	34(16)	1.8(1.0)	0.95(0.34) [32]	1.46(0.33) [34]	+14(24)	21(18)	63(17)	+68(24)	71 (9) [19]	56(10) [13]	65(12) [32]	52(19) [13]	19 (9) [19]	11 (9) [13]	16 (9) [32]	60(17) [32]																						
	Matrix transition	-44	17	42(15)	2.5(1.0)	-	-	+18(27)	23(22)	62(18)	+72(28)	-	-	-	-	-	-	-																						
	Concretion	-40	83	36(16)	3.5(1.7)	-	-	+10(37)	32(23)	52(24)	+68(40)	-	-	-	-	-	-	-																						
Li 9604 Matrix	-60	175	32(15)	1.9(1.1)	1.11(0.6) [35]	1.78(0.59) [35]	+23(38)	37(25)	59(21)	+89(37)	74(16) [19]	54(14) [16]	65(18) [35]	33(15) [16]	17(17) [19]	21(13) [16]	19(15) [35]	54(24) [35]																						
	Matrix transition	-46	91	34(18)	2.0(0.8)	-	-	+28(30)	34(23)	64(18)	+79(30)	-	-	-	-	-	-	-																						
	Concretion	-51	12	31 (8)	6.1(4.6)	-	-	0(53)	43(29)	38(30)	+96(62)	-	-	-	-	-	-	-																						

In cols. 4–19 the standard deviation is given in parentheses and the number of grains measured is given in brackets. In cols. 8–19 the angles are mean angles. Key to abbreviations: S₁, cleavage; L., length parallel to {001}; W., dimension normal to {001} (cols. 5 & 6) and normal to long dimension (col. 7); L.D., long dimension. Column 15 excludes grains with L.D. normal to {001}. The terms + or - angle, simple angle, minus angle, and plus angle are explained in the text.

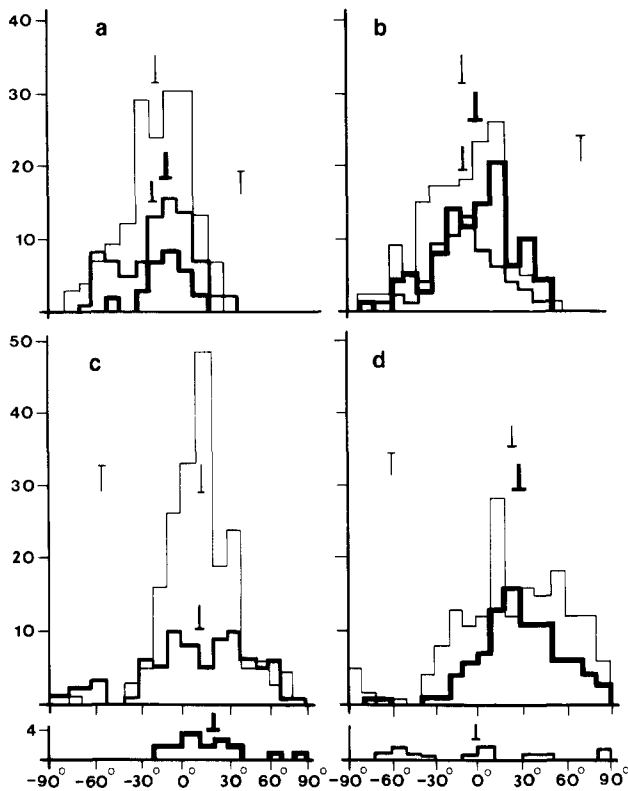


Fig. 6. Histograms plotting the number of measured chlorite–muscovite porphyroblasts (ordinate) against their angles of {001} basal cleavage with bedding (abscissa). Thin line, grains in matrix; intermediate line, grains in transition zone; thick line, grains in concretion. T indicates the angle between cleavage and bedding in the matrix; ⊥ indicates the mean values of the angle of {001} to bedding. (a) Specimen Li 9591; 1832, Nantglyn Flags. (b) Specimen Li 9593; 1834, Nantglyn Flags. (c) Specimen Li 9596; 1853, Nantglyn Flags. Histogram of the grains in the transition zone is shown below the main diagram. (d) Specimen Li 9604; 1853, Lower Ludlow Slate. Histogram of the grains in the concretion is shown below the main diagram.

Chlorite–muscovite porphyroblast analysis

I examined the relationship of porphyroblasts within four concretions and within the surrounding matrix both immediately adjacent to the concretion and up to a few centimeters away. Thin sections were cut normal to bedding and cleavage.

The following parameters were measured: length parallel to {001} and perpendicular thickness; greatest length, if different from {001}, and dimension normal to this length; angle between bedding and {001}; angle between cleavage and {001}; angle between greatest length and {001}; and angles between greatest length and bedding and greatest length and cleavage. Angles were recorded as positive or negative acute angles depending on which side of the reference direction they lay. The mean angle to the reference direction may be calculated in three ways: (1) algebraically summing the plus and minus angles, (2) converting all angles to either a plus or minus value (e.g. a -70° angle becomes a $+110^\circ$ angle) or (3) as a simple angle, that is, summing the values but ignoring the plus or minus aspect. Measurements were averaged separately for porphyroblasts in the matrix, in the transition zone, and in the concretion. The data for the four specimens are given in Table 1 and in Fig. 6. The

Li numbers refer to catalogued specimens in the petrology collection at the Field Museum of Natural History, Chicago.

The two specimens of Nantglyn Flags, Li 9591 and Li 9593, and the one of Lower Ludlow Slate, Li 9604, have ovoid calcite concretions; the one specimen from the Nantglyn Flags, Li 9596, has an ovoid siliceous concretion. Mean lengths parallel to {001} (Table 1, col. 4) are less in the matrix than in the concretion in one specimen, greater in another, and the same in two. The mean {001} L/W ratios (col. 5) are much more revealing; they are consistently less in the matrix than in the concretion.

The ratios in the matrix transition zone (col. 5) are even more interesting. In specimen Li 9593 the ratio is less than in the matrix; here the cleavage folia are more strongly developed in the portion of the transition zone where measurements were made, that is, the folia are thicker and more closely spaced. In contrast, the ratio in specimen Li 9591 is larger in the transition zone than in the matrix (also larger than in the concretion). Here the cleavage folia are similar in their degree of development to those in the matrix away from the concretion; the higher ratio may reflect the concretion producing a 'shadow effect' in the matrix. This effect may also explain the ratio being higher in the transition zone than in the general matrix of Li 9596, although it is significantly less than in the concretion. In specimen Li 9604 the ratio is nearly the same in the matrix and in the transition zone.

The mean angle of the trace of {001} to the bedding is consistently much less than the angle to cleavage in the four samples, as shown in Table 1, cols. 8–11, and in the four histograms in Fig. 6. This is evidence that the growth and orientation of the porphyroblasts are not directly related to the development and orientation of cleavage, that is, they do not lie near-parallel with the cleavage, the common orientation for phyllosilicates growing during cleavage formation. Although closer to average bedding, the mean direction generally lies at a moderate angle to it, indicating that neither mimetic crystallization nor loading perpendicular to bedding was responsible for the orientation. The mean direction of {001} for porphyroblasts within concretions is nearer bedding than it is for matrix porphyroblasts in three of the four specimens, although the standard deviation is much higher for two of these (the mean angle is also higher in these two).

Evidence of rotation of porphyroblasts during formation of cleavage is slight. Two specimens (Li 9593 and Li 9604) show the mean direction of {001} to have the smallest angle with cleavage (on a minus and on a plus angular basis, respectively) in the transition zones, where cleavage is most strongly developed (Table 1, col. 11). Specimen Li 9591 also has the smallest mean angle to cleavage in the transition zone, although here the cleavage is weakly developed for it lay in the 'shadow zone' of the concretion.

In the case of chlorite–muscovite porphyroblasts that are lozenge- or barrel-shaped rather than lath-like, I have measured their longest dimension and the width

normal to this dimension, and recorded the mean ratio of long dimension to width in Table 1, col. 7, as well as the angles between both bedding and cleavage and the longest dimension (cols. 16–19). In the matrix of all four specimens the ratio of the {001} length to width of such grains (col. 6) is significantly less than the ratio for all grains, which are more lath-like (col. 5).

The mean angle between the longest dimension and the trace of {001} (col. 15) has interesting aspects bearing on development or porphyroblast shape. In specimens Li 9596 and 9604 (Fig. 5) the longest dimension lies normal to the {001} trace in 59% and 54%, respectively, of the porphyroblasts, with their longest dimension not parallel to {001}. Such grains are somewhat unusual as they indicate growth by stacking of {001} lamellae rather than by extension parallel to cleavage, normally the easiest direction of growth.

The relationship of orientation of longest dimensions to orientation of cleavage folia in the matrix also has significance (Table 1, cols. 16–18). In all four specimens analyzed this mean angle is appreciably less than the angle between cleavage folia and the trace of {001} (col. 10). In specimen Li 9593 this angle is smallest in the transition zone where cleavage folia are more strongly developed near the concretion (col. 18). In specimens Li 9596 and Li 9604 the mean angle of {001} to cleavage in those porphyroblasts whose longest dimension is normal to {001} (col. 12) is significantly larger than the mean angle of those grains whose longest dimension is not normal to {001} (col. 13). In Li 9604 the mean angle between cleavage folia and longest dimension is smaller in those grains with their longest dimension normal to {001} (col. 16) than in the grains where it is not normal (col. 17). Porphyroblasts with their longest dimension at a high angle (including 90°) to {001} are invariably bounded by cleavage folia which have formed along the porphyroblast margins at a high angle to {001} (col. 14).

These relationships to cleavage folia suggest that the porphyroblasts have undergone a shape change during development of the folia. Such a change from the longest dimension parallel to the trace of {001}, with an orientation much closer to bedding than cleavage (the original predeformational low-grade burial metamorphism), to the longest dimension at an angle to {001} and closer to the cleavage folia orientation, could arise by dissolution of the chlorite parallel to the folia, by growth of the chlorite normal to {001}, or by both. Dissolution of the margins of grains with {001} at a moderate angle (20–30°) to the folia could produce lozenge-shaped grains; growth normal to {001} would enhance the shape change. Growth normal to {001} is, thus, one explanation for the particular morphology of these stack-like grains with their longest dimension normal to {001}.

DISCUSSION

Concretions

The distribution and degree of development of cleavage folia clearly show a relationship to the concretions.

In the Nantglyn Flag specimens with carbonate concretions, the folia are best developed in the matrix adjacent to the concretions, as shown in Fig. 1(a). Clearly, the folia formed after the concretions had developed. The matrix must have been sufficiently lithified so that dissolution cleavage folia developed normal to the direction of shortening in zones of greater strain, without the flowage that would be expected in soft sediments. Within the concretions, cleavage folia are generally restricted to a narrow margin adjacent to the zone in the matrix with more strongly developed folia, but some thin, irregular, widely spaced folia occur in the interior of some concretions.

Composition and fabric probably account for the different responses to deviatoric stress between matrix and concretion. The concretions are predominantly calcite (e.g. Li 9590 has 60% carbonate). The contrast of responses is even greater in the case of the siliceous concretions (Fig. 1b); if these represent silicified carbonate, then the silicification preceded cleavage development.

Cleavage folia are also very weakly developed in carbonate concretions in slate from the Horseshoe Pass locality, although the slate has very well-developed folia. In these specimens cleavage development in the matrix exhibits the shielding effect of the concretions; the number of folia (and thus strain) is much reduced adjacent to concretion margins that lie at a high angle to the cleavage direction. Within a narrow transition zone, at the lateral margins of a concretion, cleavage folia are prominently developed; here the composition had a higher proportion of original phyllosilicates than in the interior of the concretion (compaction had reduced pore space during concretion formation) which promoted greater development of folia. This is also reflected in the evidence for dissolution, as the calcite grains in these sections are distinctly elongate parallel to the cleavage folia.

Porphyroblasts

In the strongly cleaved zones many of the porphyroblasts have their longest dimension normal to {001} and their ratio of length parallel to {001} to width is less than the ratio for the porphyroblasts in the weakly cleaved zones. Of those grains whose longest dimension is not parallel to {001}, the angle between this dimension and cleavage is significantly less than the angle between {001} and cleavage for all porphyroblasts.

The chlorite–muscovite porphyroblasts are interpreted as having commenced growth during diagenesis. Their fresh appearance and the large mean angle of {001} to cleavage strongly support this pre-cleavage history (see, also, Craig *et al.* 1982 for a similar interpretation of porphyroblasts in similar rocks). The moderate (13–43°) mean angles of {001} to bedding suggests that bedding was not horizontal at the time the porphyroblasts nucleated and grew, particularly in the case of specimen Li 9593 (Table 1, cols. 8 & 9). Growth was a consequence of burial to a sufficient depth to promote reaction

amongst the constituents and crystallization of new phyllosilicates in equilibrium with the increasing temperature and pressure.

Davies & Cave (1976) suggested that cleavage develops during soft-sediment deformation produced by slumping or sliding of soft, completely unlithified sediments. However, analysis of the porphyroblasts clearly shows that their shape was modified during formation of cleavage folia when the rock mass was strained by deviatoric stress. The shape change was least for grains within concretions or in 'shadow zones' in the matrix caused by concretions (Li 9591); it was highest in the 'transition zones' in the region of highest strain (cleavage folia well-developed) adjacent to concretions (Li 9593). The relationship of cleavage folia to concretions on the one hand and to growth and development of the chlorite–muscovite porphyroblasts on the other hand indicates that cleavage formed during a period of deviatoric stress and moderately elevated temperature of the anchimetamorphic to lowermost greenschist facies. Thus, the fabric would have already been considerably dewatered and lithified, and cleavage development could not have taken place in soft, unlithified sediments.

Typically, phyllosilicates grow fastest parallel to {001} and thus have a sheet-like form with their longest dimensions parallel to {001}. Diagenetic grains growing during burial would have {001} planes parallel to bedding (unless the bedding was tilted during subsidence) and their longest dimensions also parallel to bedding. Likewise, chlorite grains growing during a period of deviatoric stress would be expected to have their {001} planes parallel to the greatest stretching direction, and thus parallel to any developing cleavage (normal to principal shortening).

However, on the basis of my detailed statistical studies of chlorite–muscovite porphyroblast shape and orientation, I interpret the barrel- and lozenge-shaped grains as diagenetic chlorite that has experienced shape modification by syntectonic pressure solution normal to the developing cleavage folia (that is, parallel to the finite shortening direction), but also by simultaneous growth normal to {001} and parallel to the local finite elongation direction. This would explain the occurrence of grains with their longest dimension normal to {001}.

CONCLUSIONS

The data presented for concretions, cleavage folia, and porphyroblasts from Lower Ludlow (Silurian) turbidite sequences in north-central Wales demonstrate a gradational development of cleavage folia in deformed rocks of low metamorphic grade, which is related to the degree of strain (stress). Concretions are responsible for variable folia development because they have either concentrated the strain effects in the rock matrix, resulting in well-developed cleavage folia, or produced 'strain shadows' (few or no folia). Differences in composition

between the rock matrix, narrow transition zones, and concretions have also influenced the development of cleavage folia.

The data also emphasize the importance of shape changes of chlorite porphyroblasts during the development of the cleavage folia. This was accomplished by dissolution normal to the folia and growth normal to {001} and parallel to cleavage folia.

Acknowledgements—I wish to thank Alan Woodland for help in finding localities and collecting specimens; Dorothy Eatough for preparation of thin sections and for assistance with preparing specimens for the S.E.M. and with the photography; Mary Woodland for help in the field and for critically reading and editing the manuscript; Elaine Zeiger for typing the manuscript; Z. Jastrzebski for drafting the diagrams and anonymous reviewers for critical comments on the manuscript. The Field Museum of Natural History, Chicago, supported all phases of the work.

REFERENCES

- Beach, A. 1979. Pressure solution as a metamorphic process in deformed terrigenous sedimentary rocks. *Lithos* **12**, 51–58.
- Beutner, E. C. 1978. Slaty cleavage and related strain in Martinsburg slate, Delaware Water Gap, New Jersey. *Am. J. Sci.* **278**, 1–23.
- Boswell, P. G. H. 1949. *The Middle Silurian Rocks of North Wales*. Arnold, London.
- Cobbold, P. R. 1977. Description and origin of banded deformation structures—I. Regional strain, local perturbations and deformation bands. *Can. J. Earth Sci.* **14**, 1721–1731.
- Craig, J., Fitches, W. R. & Maltman, A. J. 1982. Chlorite–mica stacks in low-strain rocks from Central Wales. *Geol. Mag.* **119**, 243–256.
- Cummins, W. A. 1959. The Nantglyn Flags; mid-Salopian basin facies in Wales. *Lpool & Manch. geol. J.* **2**, 159–167.
- Davies, W. & Cave, R. 1976. Folding and cleavage determined during sedimentation. *Sediment. Geol.* **15**, 89–133.
- Gray, D. R. 1978. Cleavages in deformed psammitic rocks from southeastern Australia: their nature and origin. *Bull. geol. Soc. Am.* **89**, 577–590.
- Gray, D. R. 1979. Microstructure of crenulation cleavages: an indicator of cleavage origin. *Am. J. Sci.* **279**, 97–128.
- Groshung, R. H., Jr. 1975. "Slip" cleavage caused by pressure solution in a buckle fold. *Geology* **3**, 411–413.
- Knipe, R. J. & White, S. H. 1977. Microstructural variation of an axial plane cleavage around a fold—a H.V.E.M. study. *Tectonophysics* **39**, 355–380.
- Piqué, A. 1982. Relations between stages of diagenetic and metamorphic evolution and the development of a primary cleavage in the north-western Moroccan Meseta. *J. Struct. Geol.* **4**, 491–500.
- Plessman, W. 1964. Gesteinlösung, ein Hauptfaktor beim Schieferungsprozess. *Geol. Mitt.* **4**, 69–82.
- Reks, I. J. & Gray, D. R. 1983. Strain patterns and shortening in a folded thrust sheet: an example from the southern Appalachians. *Tectonophysics* **93**, 99–128.
- Roy, A. B. 1978. Evolution of slaty cleavage in relation to diagenesis and metamorphism: a study from the Hunsrückschiefer. *Bull. geol. Soc. Am.* **89**, 1775–1785.
- Talbot, G. L. 1965. Crenulation cleavage in the Hunsrückschiefer of the middle Moselle region. *Geol. Rdsch.* **54**, 1026–1043.
- Weber, K. 1981. Kinematic and metamorphic aspects of cleavage formation in very low-grade metamorphic slates. *Tectonophysics* **78**, 291–306.
- White, S. H. & Knipe, R. J. 1978. Microstructure and cleavage development in selected slates. *Contr. Miner. Petrol.* **66**, 165–174.
- Williams, P. F. 1972. Development of metamorphic layering and cleavage in low-grade metamorphic rocks at Bermagui, Australia. *Am. J. Sci.* **272**, 1–47.
- Woodland, B. G. 1982. Gradational development of domainal slaty cleavage, its origin and relation to chlorite porphyroblasts in the Martinsburg Formation, Eastern Pennsylvania. *Tectonophysics* **82**, 89–124.